

Mobility Robustness Optimization based on Radio Link Failure Prediction

Yi-Wei Ma^{1,*}, Jiann-Liang Chen² and Hao-Kai Lin²

¹China Institute of FTZ Supply Chain, Shanghai Maritime University, China

²Department of Electrical Engineering, National Taiwan University of Science & Technology, Taipei, Taiwan

*yiweimaa@gmail.com

Abstract — This work proposes a Mobility Robustness Optimization (MRO) mechanism that is based on radio link failure prediction, called MBRP, for dealing with Radio Link Failures (RLFs) during the handover process. This work concerns these handover failures, considers a parameter that is defined in 3GPP- A3 offset, and derives models of handover between cells. The proposed Mobility Robustness Optimization based on Radio Link Failure Prediction (MBRP) mechanism is compared with the HO-region and reduces the number of RLFs by 1.08%.

Index Terms — Mobility Robustness Optimization, Self-Organizing Network, Radio Link Failure

I. INTRODUCTION

To change repeatedly the operating conditions and topology of a network, efficient ways of dealing with these parameters are required to keep the network stable and reliable. Interrelated serving costs are extremely high [1-3].

The development of the Self-Organizing Network (SON) [2-4], based on 3GPP network providing “plug and play” functionality in eNBs and small cells. SON to configure automatically and adapt varying radio channel [5]. MRO was examined a use case for self-organization networks to reduce the numbers of RLFs and unnecessary handovers. Data rates of tens of megabits per second should be supported for many users. As the number of base stations increases, UEs that are moving on same trajectory encounter more handovers, increasing traffic and, therefore, the number of RLFs [6-10].

II. PROPOSED MBRP SYSTEM ARCHITECTURE

A. System Overview

This work proposes a Mobility Robustness Optimization (MRO) mechanism that is based on radio link failure prediction, for dealing with Radio Link Failures (RLFs) during the handover process. In the proposed system architecture, each operational module is composed of a monitoring module, a Mobility Robustness Optimization based on Radio Link Failure Prediction (MBRP) mechanism module and an RLF threshold comparison module. MRO is one of the functions of SON that deals with three types of RLF. The MBRP mechanism calculates optimal parameters and optimizes a cell. The proposed RLF threshold comparison module sends information about any base station for which the number of RLFs exceed the RLF threshold to the MBRP mechanism. Figure 1 shows proposed system architecture, showing the main modules that are relevant to this work.

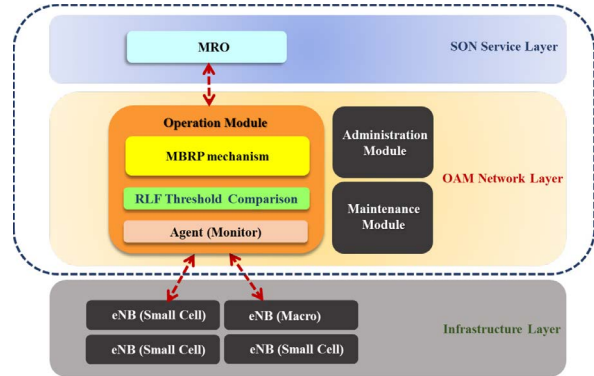


Figure 1. The proposed MBRP system architecture

Figure 2 shows the operating time sequence of MBRP System. The device sends its operation information to OAM. The monitoring module receives handover information (too early, too late, or wrong cell) and the positions of UEs and the cell. It then sends information to the RLF threshold comparison module, which in turn sends information (concerning any base station whose number of RLFs exceeds the RLF threshold) to the MBRP mechanism. Finally, the MBRP mechanism calculates the optimal parameters and optimizes the cell.

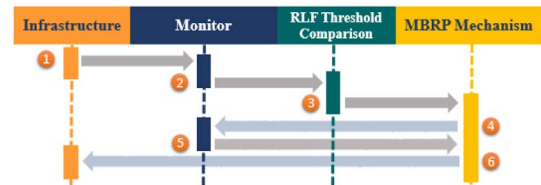


Figure 2. The time sequence of MBRP System

B. Monitor

For a MRO, the architecture must include data that are gathered automatically by network monitoring. The monitoring module receives the position of a small cell, the number of its RLFs, the number of UEs under the network, the positions of the UEs, the position of the macro cell and the number of its RLFs. After it has received this information, the monitoring module sends it to the RLF threshold comparison module.

C. RLF Threshold Comparison

First, the monitoring module receives the numbers of RLFs of the base stations, the positions of the base stations, and the positions of users. Second, a threshold value is defined. If the number of RLFs of a cell exceeds the threshold, then the cell will be marked. The mechanism autonomously compares the

numbers of RLFs of every cell in the network against a threshold, and sends information about the marked cells to the MBRP mechanism to enable to be calculated.

Figure 3 shows a flow chart of the of the RLF threshold comparison procedure. First, the system loads information about the base stations from the monitoring module. Second, it compares the number of RLFs of the base stations with the RLF threshold. In the next step, the system marks the base stations for which the number of RLFs exceeds the RLF threshold. When a comparison has been performed for every base station, the system executes the MBRP mechanism.

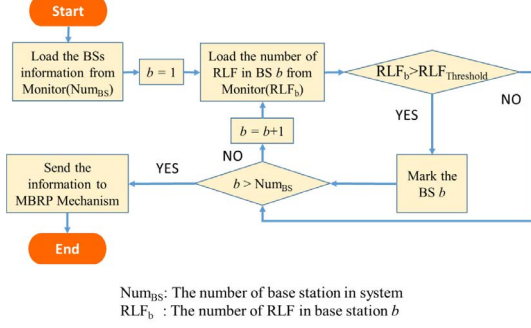


Figure 3. The flowchart of RLF Threshold Comparison

D. MBRP Mechanism

The proposed MBRP mechanism adjusts the A3 offset of a cell to reduce the number of RLFs. If the SINR value of a serving cell exceeds the value of Q_{out} , then no RLF will occur, and UE can connect to a cell. Similarly, the SINR value of the target cell exceeds the value of Q_{out} , then no RLF will occur, and UE can connect to a cell. Restated, when a UE is connected to a serving cell and its SINR value is less than Q_{out} , an RLF will occur. When a UE is connected to a target cell and its SINR value is lower than Q_{out} , then an RLF will also occur. A function of distance between a UE and a cell can be generated from two functions (as shown in fig. 4), and this distance function is substituted into last two functions, as shown in fig. 4. Therefore, the value of A3offset can be obtained from its relationship. The system retrieves A3offset values that exceeds -15dB and a lower than 15dB. Similarly, A3offset can be evaluated using this relationship. Finally, the MBRP mechanism doubles the average of all A3offset values, rounds it up or down, and then divides this value by two. $RSRP_{u,i}$ is UE u receive Reference Signal Received Power from Cell i . In this work, the value of Cell Individual Offset (CIO) and the hysteresis are set to zero. Equations (1) and (2) shows the calculations that are made as part of the MBRP mechanism. Figure 5 shows the corresponding flowchart.

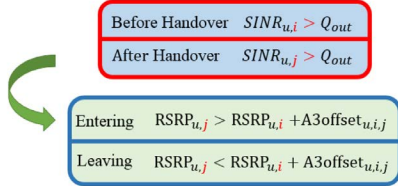


Figure 4. The function of MBRP Mechanism

$$CIO_j - hys > RSRP_{u,i} + CIO_i + A3offset_{0\ u,i,j} \quad (1)$$

$$RSRP_{u,j} + CIO_j + hys < RSRP_{u,i} + CIO_i + A3offset_{0\ u,i,j} \quad (2)$$

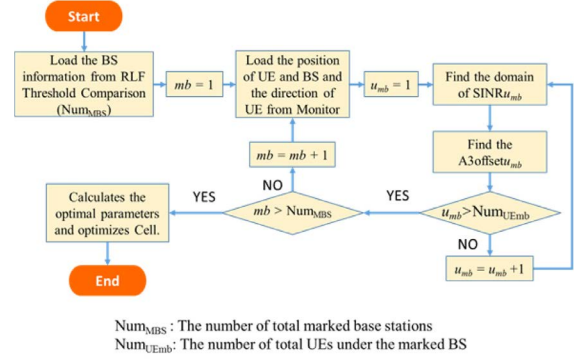


Figure 5. The flowchart of MBRP Mechanism

III. PERFORMANCE ANALYSIS

A. The Number of RLFs

As described in the preceding section, every period, three RLF conditions are recorded which of the three RLF conditions applies is recorded. Table 1. shows the RLFs in two simulated scenarios, described above.

Table 1. The number of RLF

	Too early	Too late	Wrong cell	Total RLF	Total HO
10 Per Macro	22	278	132	432	5267
	5.092593%	64.35185%	30.55556%	8.215%	
20 Per Macro	44	575	330	949	7496
	4.636459%	60.59009%	34.77345%	12.67%	

Figure 6 compares the uses of the existing MRO methods in the two scenario.

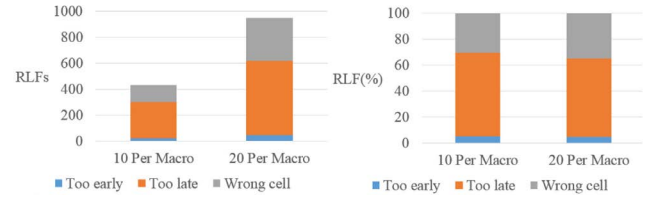


Figure 6. The number of RLF

B. A3 Offset of the System

This work compares A3 offsets of system in two simulated scenarios. Figure 7 shows the A3 offset values of system. The dotted line represents the mean A3offset values that are obtained by applying the proposed MBRP mechanism in the second scenario, and the solid line represents the mean A3offset values that are obtained by applying the proposed MBRP mechanism in the first scenario. The second scenario yields better A3offset values, which are obtained more quickly, than the first scenario.

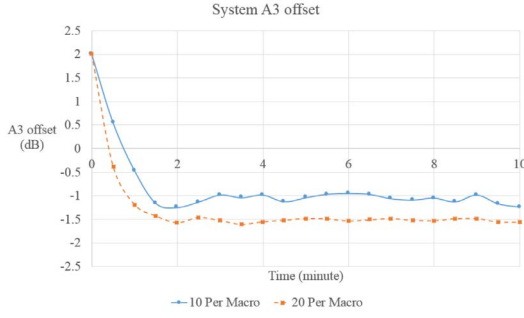


Figure 7. The A3 offset value of system

C. A3 Offset of the base station

This work compares the A3offsets of a macro cell in two scenarios. Figures 8 and 9 plot the A3offset values of system. The dotted line represents the mean A3offset values that are obtained by applying the proposed MBRP mechanism in the second scenario, and the solid line represents the mean A3offset values that are obtained by the applying proposed MBRP mechanism in the first scenario. The second scenario yields better A3offset values faster than the first scenario.

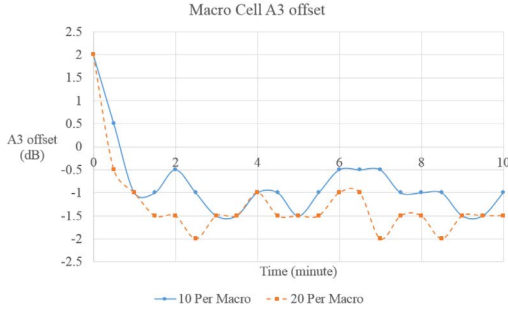


Figure 8. The A3 offset value of Macro Cell

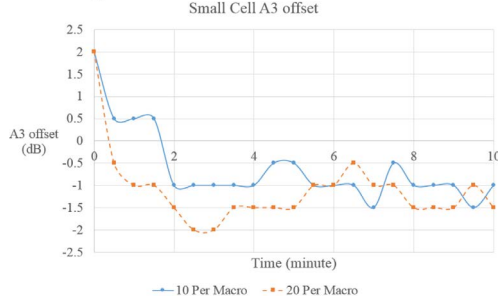


Figure 9. The A3 offset value of Small Cell

D. Compare with HO-region

The proposed MBRP mechanism is compared with the HO-region [11]. Figures 10 and 11 shows the that proposed mechanism in this study reduces the number of RLFs by 1.08%. The HO-region method does not collect the RLF of the overall simulation time nor does it collect the RLF of a time unit, so the RLF of percentage of the HO-region is fixed as 6.2%. The proposed MBRP mechanism is compared with the HO-region is shown in below.

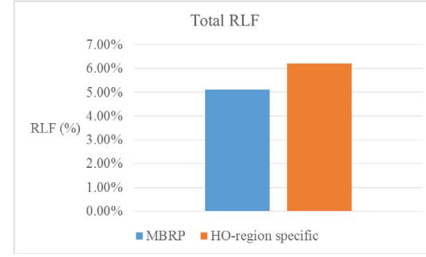


Figure 10. The total RLF of applying MBRP and HO-region specific

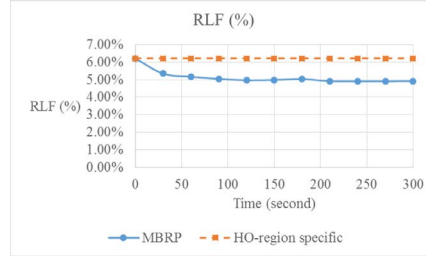


Figure 11. The total RLF of applying MBRP and HO-region specific in the computing period

IV. CONCLUSION

This work developed and simulated a novel SON solution for optimizing radio link failure among small cells and macro cells. The results herein demonstrate that the decrease in the total number of radio link failures that is achieved using the proposed novel MRO-based algorithm indicates that the SON solution outperforms. The MBRP algorithm periodically receives information about the position of UE, and inputs it into the proposed formula to improve the A3offset values. The simulation results herein demonstrate that the number of RLFs after the MBRP mechanism is used is 1.08% lower than that after the HO-region mechanism is used, allowing the system to reach a steady state in a short time.

REFERENCES

- [1] I.Z. Kovacs, D. Laselva, P.H. Michaelsen, Y. Wang, R. Djapic and K. Spaey, "Performance of SON for RSRP-based LTE/WLAN access network selection," *Proceedings of the International Symposium on Wireless Communications Systems*, pp.360-364, 2014.
- [2] I.G. Ben Yahia, C. Destre and A. Quenot, "Scenarios for eNodeB and SON functions programmability," *Proceedings of the IEEE in Wireless Communications and Networking Conference Workshops*, pp.208-212, 2014.
- [3] S. Hahn and T. Kurner, "Managing and altering mobile radio networks by using SON function performance models," *Proceedings of the International Symposium on Wireless Communications Systems*, pp.214-218, 2014.
- [4] C. Schmelz, S. Hahn, A. Eisenblatter, S. Lohmuller, C. Frenzel and T. Kurner, "SON management demonstrator," *Proceedings of the IEEE in Network Operations and Management Symposium*, pp.1-2, 2014.
- [5] The Mobile Broadband Standard, 3GPP SON., Retrieved March 12, 2017, from <http://www.3gpp.org/technologies/keywords/acronyms/105-son>
- [6] G.K. Chang, C. Liu and L. Zhang, "Architecture and applications of a versatile small-cell, multi-service cloud radio access network using radio-over-fiber technologies," *Proceedings of the IEEE in Communications Workshops*, pp.879-883, 2013.
- [7] G. Bartoli, R. Fantacci, K. Letaief, D. Marabissi, N. Privitera, M. Pucci and J. Zhang, "Beamforming for small cell deployment in LTE-advanced and beyond," *Proceedings of the IEEE in Wireless Communications*, pp.50-56, 2014.
- [8] K. Suto, H. Nishiyama and N. Kato, "Postdisaster User Location Maneuvering Method for Improving the QoE Guaranteed Service Time in Energy Harvesting Small Cell Networks," *IEEE Transactions on Vehicular Technology*, vol. 66, no. 10, pp. 9410-9420, Oct. 2017.
- [9] H. Zhang, H. Li, J. H. Lee and H. Dai, "QoS-Based Interference Alignment With Similarity Clustering for Efficient Subchannel

- Allocation in Dense Small Cell Networks," *IEEE Transactions on Communications*, vol. 65, no. 11, pp. 5054-5066, 2017.
- [10] J. Moysen and L. Giupponi, "Self Coordination among SON Functions in LTE Heterogeneous Networks," *Proceedings of the IEEE in Vehicular Technology Conference*, pp.1-6, 2015.
- [11] W. Gao, B. Jiao, G. Yang, W. Hu, L. Chi and J. Liu, "Mobility robustness improvement through transport parameter optimization in HetNets," *Proceedings of the IEEE International Symposium on Personal, Indoor and Mobile Radio Communications*, pp. 101-105, 2013.